FIRST RESULTS OF ATMOSPHERIC COMPOSITION RETRIEVAL USING IASI-METOP AND AIRS-AQUA DATA

Franz Schreier[1], Michal Szopa[1], Adrian Doicu[1], Sebastián Gimeno-García[1], Christine Böckmann[2], and Peter Hoffmann[3]

[1]*DLR — German Aerospace Center, Remote Sensing Technology Institute, Oberpfaffenhofen, 82234 Wessling, Germany (franz.schreier, michal.szopa, adrian.doicu, Sebastian.GimenoGarcia@dlr.de)*
[2]*University of Potsdam, Institute of Mathematics, 14469 Potsdam, Germany (bockmann@rz.uni-potsdam.de)*
[3]*University of Leipzig, Institute for Meteorology, 04103 Leipzig, Germany (phoffma@rz.uni-leipzig.de)*

ABSTRACT

Regularization methods for the inversion of infrared nadir sounding observations are currently investigated. An iterative Runge-Kutta type method for nonlinear ill-posed problems has been implemented and its performance has been studied using synthetic measurements. Comparisons with Tikhonov type inversion with a priori regularization parameter selection indicate that both methods are of similar accuracy; however, the Runge-Kutta method is less sensitive to regularization parameter variations.
Furthermore, vertical column density retrieval from nadir infrared sounders such as AIRS will be used for validation of column densities retrieved from near infrared SCIAMACHY observations. Two closely related retrieval codes are used for L2 processing of SCIAMACHY near infrared and AIRS mid infrared spectra. First results of this intercomparison are shown.

Key words: New algorithms and products, regularization, IASI, AIRS, SCIAMACHY.

1. INTRODUCTION

Atmospheric remote sensing with space borne nadir viewing infrared spectrometers has become indispensable to gain information relevant for weather forecasting and trace gases relevant for climate as well as air quality. Unfortunately the inversion, i.e., the retrieval of atmospheric state parameters ("level 2" data) from the spectroscopic observations ("level 1"), is an ill-posed problem, and additional information has to be provided in order to obtain useful results. In the atmospheric science community "Optimal Estimation" [1] has been in widespread use for many years, whereas Tikhonov regularization [2] has gained attraction only in the past decade [e.g. 3, 4, 5]. While Tikhonov regularization for linear inverse problems is well established [6], nonlinear problems are still challenging and an active field of mathematical research. In section 2 we present an alternative approach based on Runge–Kutta methods, and show first results using synthetic SCIAMACHY and IASI spectra.

Verification and validation is mandatory in computational science [7]. and has been established as an integral part of (the assessment of) all atmospheric sounding missions. Whereas verification ("Is the code correct?") is frequently performed by means of code intercomparisons [e.g., 8, 9], a comparison of retrieval results with independent characterizations of the atmospheric state is essential for validation ("Is it the correct code?"). Clearly the true state of the atmosphere is difficult to obtain, so comparisons with retrievals using other remote sensing instruments are frequently used. In section 3 we discuss our approach to validate carbon monoxide remote sensing using SCIAMACHY and AIRS nadir sounders.

2. REGULARIZATION

The standard approach to estimate the unknown $\boldsymbol{x}$ from a measurement vector $\boldsymbol{y}$ relies on (nonlinear) least squares

$$\min_x \|\boldsymbol{y} - \boldsymbol{F}(\boldsymbol{x})\|^2 \tag{1}$$

Here $\boldsymbol{F}$ denotes the forward model, and the unknown state vector $\boldsymbol{x}$ is comprised of the geophysical and auxiliary (e.g., instrumental) parameters. Typically, only noisy data are available due to measurement errors; we therefore distinguish the "correct" data $\boldsymbol{y}$ from the available noisy data $\boldsymbol{y}^\delta = \boldsymbol{y} + \boldsymbol{\delta}$. Likewise, only an estimate $\boldsymbol{x}^\delta$ of the correct state vector $\boldsymbol{x}$ can be obtained.

Because of the ill-posed nature of vertical sounding inverse problems, regularization is indispensable, i.e.,

$$\min_x \left(\|\boldsymbol{y} - \boldsymbol{F}(\boldsymbol{x})\|^2 \; + \; \lambda \, \|\mathsf{L}(\boldsymbol{x} - \boldsymbol{x}_\mathrm{a})\|^2 \right) \tag{2}$$

where $\boldsymbol{x}_\mathrm{a}$ is an a priori state vector, L is a regularization matrix, and λ is a regularization parameter.

For linear inverse problems Tikhonov regularization with various parameter choice methods (e.g., L–curve,

Proc. '2nd EPS/MetOp RAO Workshop', Barcelona, Spain
20-22 May 2009, (ESA SP-675, September 2009)

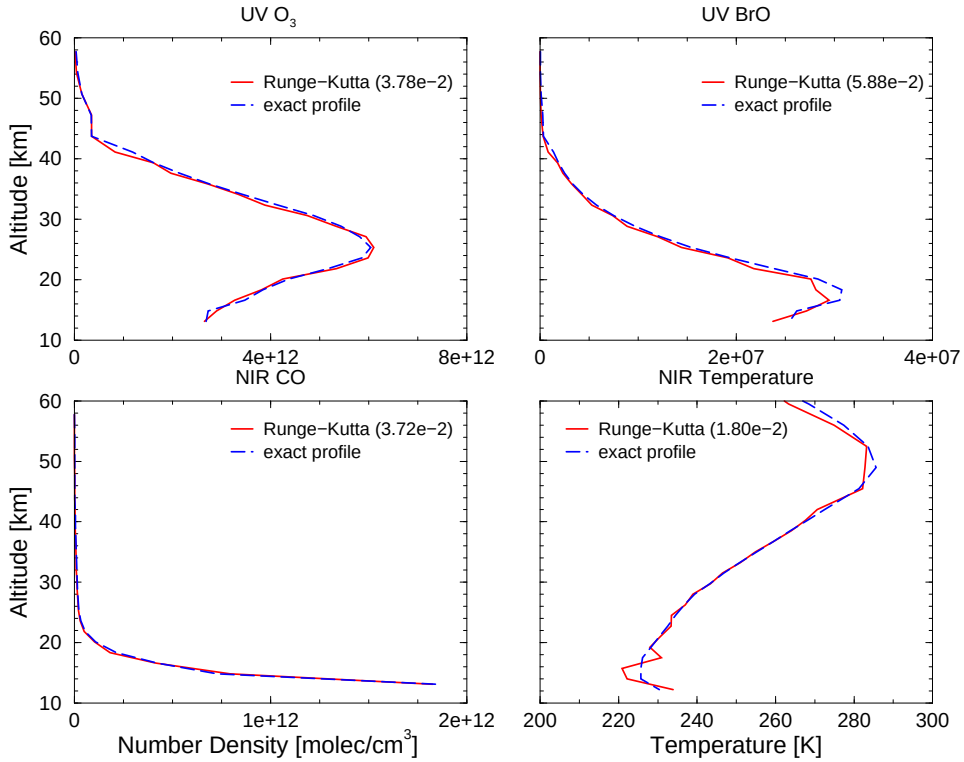

Figure 1. Comparison of profiles retrieved with the Runge–Kutta regularization scheme with the exact profile for the SCIAMACHY limb sounding test cases.

GCV, ...) has been used extensively. For nonlinear Tikhonov regularization the "Iteratively Regularised Gauss-Newton" (IRGN) method and the regularized Levenberg-Marquardt method have been utilized as efficient solvers [10, 11]. These and further methods have been implemented in the DRACULA (aDvanced Retrieval Atmosphere Constrained & Unconstrained Least squares Algorithms) library [12].

2.1. Runge–Kutta Regularization

The Runge-Kutta method is a popular family of algorithms for solving initial value problems (IVP). Applied to a problem of the form $\dot{\boldsymbol{x}}(t) = \Psi(t, \boldsymbol{x}(t))$ with $\boldsymbol{x}(0) = \boldsymbol{x}_0$ it is characterized by the following iterative procedure:

$$\boldsymbol{x}_{k+1} = \boldsymbol{x}_k + \tau_k \sum_{i=1}^{s} b_i \Psi(t + c_i\tau_k, \boldsymbol{v}_i), \tag{3}$$

$$\boldsymbol{v}_i = \boldsymbol{x}_k + \tau_k \sum_{j=1}^{s} a_{ij} \Psi(t + c_j\tau_k, \boldsymbol{v}_j) \tag{4}$$

with method-specific parameters $\mathsf{A} \equiv (a_{ij}) \in \mathbb{R}^{s\times s}$, $\boldsymbol{b} \equiv (b_1 \dots b_s)^T \in \mathbb{R}^{s\times 1}$, and $\boldsymbol{c} \equiv (c_1 \dots c_s)^T \in \mathbb{R}^{s\times 1}$.

Tautenhahn [13] has shown that solving a nonlinear inverse problem $\boldsymbol{F}(\boldsymbol{x}) = \boldsymbol{y}$ is equivalent to solving an IVP

$$\begin{aligned} \dot{\boldsymbol{x}}^\delta(t) &= \mathsf{K}^T(\boldsymbol{x}^\delta(t))[\boldsymbol{y}^\delta - \boldsymbol{F}(\boldsymbol{x}^\delta(t))], \qquad 0 < t < T, \\ \boldsymbol{x}^\delta(0) &= \boldsymbol{x}_a \end{aligned} \tag{5}$$

where K is the Jacobian. This differential equation can be readily solved using the Runge–Kutta formalism [14], where T plays the role of a regularization parameter. Applying the two stage ($s = 2$) scheme to (5) results in

$$\boldsymbol{x}^\delta_{k+1} \;=\; \boldsymbol{x}^\delta_k + \tilde{\boldsymbol{b}}^{\mathrm{T}} \Big(\alpha_k \mathsf{I}_{2n} + \mathsf{B}_k\Big)^{-1} \boldsymbol{s}^\delta_k \tag{6}$$

where $\alpha_k = \frac{1}{\tau_k}$ is the inverse step length, and

$$\tilde{\boldsymbol{b}} \;=\; \boldsymbol{b} \otimes \mathsf{I}_n \tag{7}$$

$$\boldsymbol{s}^\delta_k \;=\; \begin{pmatrix} \mathsf{K}^{\mathrm{T}}_k \big(\boldsymbol{y}^\delta - \boldsymbol{F}(\boldsymbol{x}^\delta_k)\big) \\ \mathsf{K}^{\mathrm{T}}_k \big(\boldsymbol{y}^\delta - \boldsymbol{F}(\boldsymbol{x}^\delta_k)\big) \end{pmatrix} \tag{8}$$

$$\mathsf{B}_k \;=\; \begin{pmatrix} a_{11} & a_{12} \\ a_{21} & a_{22} \end{pmatrix} \otimes \mathsf{K}^{\mathrm{T}}_k \mathsf{K}_k \,. \tag{9}$$

Here I_n denotes an $n \times n$ identity matrix, and the Kronecker product for two matrices $\mathsf{A} = (a_{ij}) \in \mathbb{R}^{m\times n}$ and $\mathsf{B} \in \mathbb{R}^{k\times p}$ is defined as

$$\mathsf{A} \otimes \mathsf{B} \;=\; \begin{pmatrix} a_{11}\mathsf{B} & \dots & a_{1n}\mathsf{B} \\ \vdots & \ddots & \vdots \\ a_{m1}\mathsf{B} & \dots & a_{mn}\mathsf{B} \end{pmatrix} \tag{10}$$

Numerical implementations of the 1- and 2-stage RK-type iterative regularization methods along with three test cases are described in [14]. Recently, this method has also been added to the DRACULA library.

2.2. Results

The Runge-Kutta regularization has been tested with synthetic spectra for both limb and nadir passive atmospheric soundings, including comparisons with the Tikhonov-type methods with a priori regularization parameter.

SCIAMACHY on Envisat is observing the Earth in nadir, limb, and occultation mode in eight channels covering the ultraviolet (UV) to the near infrared (NIR) [15]. For these tests limb observations of ozone (wavelength $520-580\,\mathrm{nm}$) and BrO ($337-357\,\mathrm{nm}$) in the UV and carbon monoxide (wavenumber $4180-4205\ \mathrm{cm}^{-1}$) in the NIR were simulated. A limb sequence starting at a tangent altitude of $13.6\,\mathrm{km}$ with $\Delta h_{\mathrm{t}} = 3.3\,\mathrm{km}$ was assumed. Gaussian noise has been added: SNR=300 for O_3 and 10^3 for BrO and CO. The NIR spectra were also used to test the performance of various regularization methods for temperature sounding (with SNR=10^4). In Fig. 1 a comparison of Runge-Kutta retrieval results with the exact profile used to generate the synthetic measurements is shown. The relative error $\|\boldsymbol{x}^{\delta} - \boldsymbol{x}^{\mathrm{true}}\|/\|\boldsymbol{x}^{\mathrm{true}}\|$ and the number of iterations for O_3 and BrO as a function of the regularization strength p are shown in Fig. 2.

Synthetic IASI spectra in the wavenumber range $1000-1070\ \mathrm{cm}^{-1}$ were used to test the new scheme for nadir infrared sounding. Gaussian noise with SNR=1000 was added to the synthetic spectra; H_2O and CO_2 were considered as interfering species. Fig. 3 shows the performance of the Runge–Kutta scheme compared to the nonlinear Tikhonov regularization method.

In conclusion, the Runge-Kutta method seems to yield results of similar precision as the Tikhonov-method while being less dependent on variations of the regularization parameter. Further tests with real measurement data are required before final conclusions can be drawn.

3. INTERCOMPARISON OF SCIAMACHY AND AIRS CARBON MONOXIDE

Nadir observations in the shortwave infrared channels of SCIAMACHY [15] onboard the ENVISAT satellite can be used to derive information on CO, CH_4, N_2O, CO_2, and H_2O, e.g., profiles of volume mixing ratio $q_X(z)$ or density $n_X(z) = q_X(z) \cdot n_{\mathrm{air}}(z)$ of molecule X. Unfortunately, the analysis of the NIR channels of SCIAMACHY is challenging because of

— tiny signal on huge background;
— ice layer on channel 8 detector;
— increasing number of dead and bad pixels;
— CO and N_2O retrieval: very weak absorbers

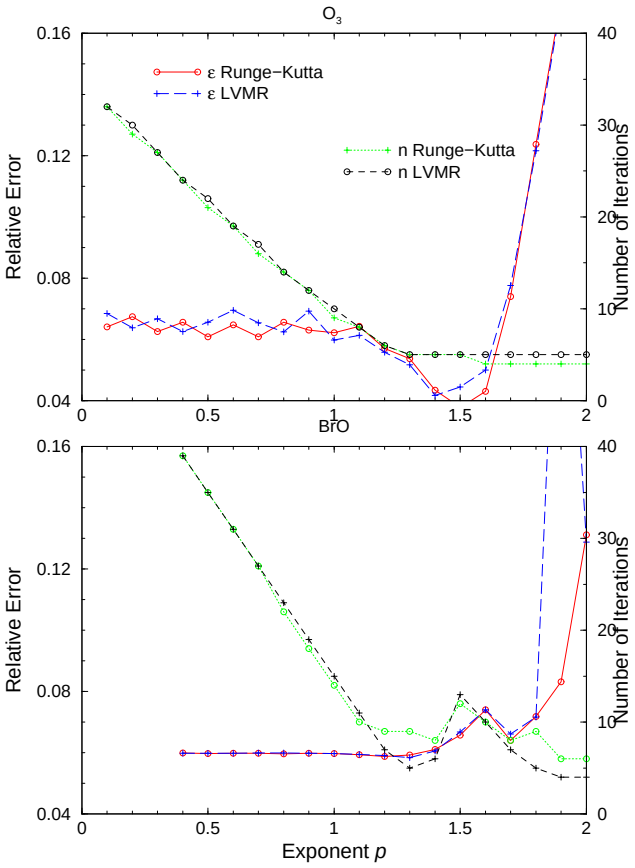

Figure 2. Runge–Kutta vs regularized Levenberg-Marquardt for the SCIAMACHY limb UV test cases. The regularization parameter is chosen as $\alpha = \sigma^p$ where σ is the noise standard deviation. Note that a small exponent p corresponds to strong regularization.

Furthermore vertical sounding inversions are ill-posed, so it is customary to retrieve only column densities (VCD)

$$N_X \equiv \int_{z_{\mathrm{ground}}}^{\infty} n_x(z)\,\mathrm{d}z\,. \qquad (11)$$

For UV instruments such as SCIAMACHY the analysis is traditionally based on a DOAS methodology, and this approach has also been successfully applied to SCIAMACHY's near infrared channels [16, 17].

To gain greater flexibility and to have a robust and efficient inversion for the operational level 2 data processing, a new code "BIRRA" (Beer InfraRed Retrieval Algorithm) has been developed at DLR. In the framework of code verification and validation, a careful intercomparison of BIRRA carbon monoxide VCD's with data retrieved by University of Bremen's WFM-DOAS and SRON's IMLM [18] codes has been performed [19]. Moreover, molecular column densities retrieved from infrared atmospheric soundings have been compared [20].

In view of the similarities between column density retrievals in the near and mid infrared, a modified version

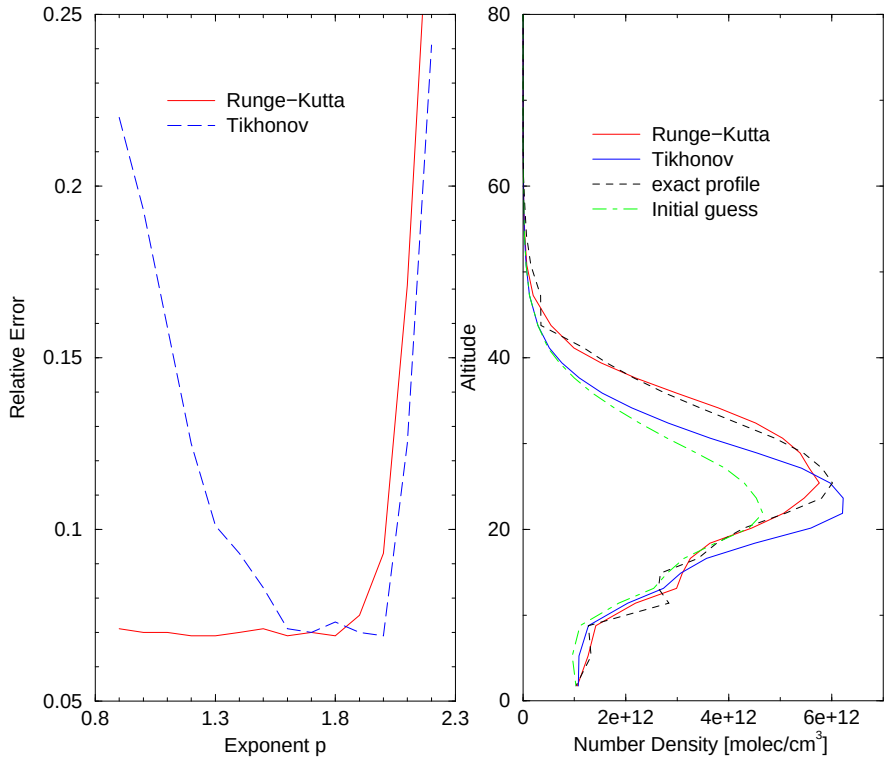

Figure 3. Comparison of Runge–Kutta versus Tikhonov regularization scheme for ozone retrievals in the infrared with a synthetic IASI spectrum.

of BIRRA called CERVISA (Column EstimatoR Vertical Infrared Sounding of the Atmosphere) has been implemented recently for level 1 $\rightarrow$ 2 processing of nadir thermal infrared sounding data. For the nonlinear least squares problem (1) BIRRA and CERVISA use solvers of the PORT Optimization Library [21] based on a scaled trust region strategy. Optionally a least squares with simple bounds (to prevent, e.g., negative values for physical parameters) or a separable nonlinear least squares solver can be used.

3.1. Near vs Mid Infrared Radiative Transfer

The BIRRA and CERVISA forward model is based on MIRART/GARLIC [22], a line-by-line code for arbitrary observation geometry (up, down, limb) and instrumental field-of-view and line shape that provides Jacobians by means of automatic differentation [23] and has been verified in extensive intercomparisons [e.g. 8, 24].

The intensity (radiance) I at wavenumber ν received by an instrument at $s = 0$ is described by the equation of radiative transfer [25]

$$I(\nu) \;=\; I_{\rm b}(\nu)\,\mathcal{T}(\nu) - \int_0^\infty {\rm d}s'\, J(\nu,s)\,\frac{\partial \mathcal{T}(\nu;s')}{\partial s'}, \quad (12)$$

where $\mathcal{T}$ is transmission, $I_{\rm b}$ is a background contribution, and J is the source function. The instrument is taken into account by convolution of the monochromatic intensity spectrum (12) with an spectral response function $\mathcal{S}$.

In the near infrared, reflected sunlight becomes important, whereas thermal emission is neglegible. For clear sky observations scattering can be neglected, hence

$$\begin{aligned} I(\nu) \;&=\; r(\nu)\; I_{\rm sun}(\nu)\; \mathcal{T}_\uparrow(\nu)\, \mathcal{T}_\downarrow(\nu) \qquad (13)\\ &=\; r I_{\rm sun} \times \exp\left[-\int_0^\infty \frac{{\rm d}z'}{\mu} \sum_m \alpha_m \bar{n}_m(z')\, k_m(\nu,z') \right] \\ &\quad \times \exp\left[-\int_0^\infty \frac{{\rm d}z''}{\mu_\odot} \sum_m \alpha_m \bar{n}_m(z'')\, k_m(\nu,z'') \right] \end{aligned}$$

where r is reflection (albedo) and $\mathcal{T}_\uparrow$ and $\mathcal{T}_\downarrow$ denote transmission between reflection point (e.g. Earth surface at altitude $z_{\rm b}$) and observer and between sun and reflection point, respectively. k_m and $\bar{n}_m(z)$ are the (pressure and temperature dependent) absorption cross section and reference (e.g., climatological) density of molecule m, and α_m are the scale factors to be estimated. (Note that for simplicity we have used a plane–parallel approximation with $\mu \equiv \cos\theta$ for an observer zenith angle θ and $\mu_\odot$ for the solar zenith angle $\theta_\odot$; moreover continuum is neglected here.)

In the mid (thermal) infrared solar irradiance can be neglected, and the signal is a combination of attenuated sur-

face emission and thermal emission of the atmosphere,

$$
\begin{aligned}
I(\nu) &= \epsilon(\nu)\, I_{\text{surf}}(\nu)\, \mathcal{T}_{\uparrow}(\nu) + I_{\text{atm}}(\nu) \\
&= \epsilon(\nu)\, B(\nu, T_{\text{surf}})\, \mathcal{T}_{\uparrow}(\nu) \\
&\quad + \int_0^{\tau} B(\nu, T(\tau))\, \exp\left(-\tau'(\nu)\right) \mathrm{d}\tau'
\end{aligned}
\tag{14}
$$

where τ denotes optical depth ($\mathcal{T} = \mathrm{e}^{-\tau}$) and $\epsilon = 1 - r$ denotes surface emissivity.

3.2. Carbon monoxide retrievals: data and assumptions

Carbon monoxide is an important trace gas affecting air quality and climate and highly variable in space and time. About half of the CO comes from anthropogenic sources (e.g., fuel combustion), and further significant contributions are due to biomass burning. CO is a target species of several spaceborne instruments, nb. AIRS, MOPITT, and TES from NASA's EOS satellite series, and MIPAS and SCIAMACHY on ESA's Envisat.

This intercomparison is based on SCIAMACHY Level 1c data of orbit 8663 (27. October 2003) covering Russia, the Arabic peninsula, and Eastern Africa. In this observation period large biomass fire existed esp. in Mozambique, which should be clearly visible in CO column densities derived from nadir sounding instruments.

For the retrieval of carbon monoxide vertical column densities with BIRRA, level 1 data of SCIAMACHY channel 8 applying the Bremen bad/dead pixel mask have been used; hence a single spectrum comprises 51 data points in the interval 4282.686 to $4302.131\,\mathrm{cm}^{-1}$. Surface reflectivity was modelled with a second order polynomial, baseline was ignored. Scaling factors for CO, CH_4, and H_2O were fitted along with the Gaussian slit function half widths and the reflectivity coefficients.

CO column density retrievals from AIRS were performed for three orbits (7868, 7889, and 7996 at October 26, 27, and 28) passing over Mozambique. Note that the October 26 and 28 data originate from dayside observations, whereas orbit 07889 is nighttime. In accordance with McMillan et al. [26] the $2181-2220\ \mathrm{cm}^{-1}$ microwindow containing 42 spectral points was used. In addition to scaling factors for CO, CO_2, H_2O, and N_2O surface temperature was considered as unknown.

Pressure and temperature profiles were read from the CIRA dataset [27], providing monthly mean values for the altitude range $0-120\,\mathrm{km}$ with almost global coverage (80N – 80S in 5dg steps). Trace gas concentrations were taken from a coarse resolution version of the US standard atmosphere [28]. Molecular absorption was modelled using the HITRAN2004 database [29] (with updates for H_2O) along with the CKD continuum corrections.

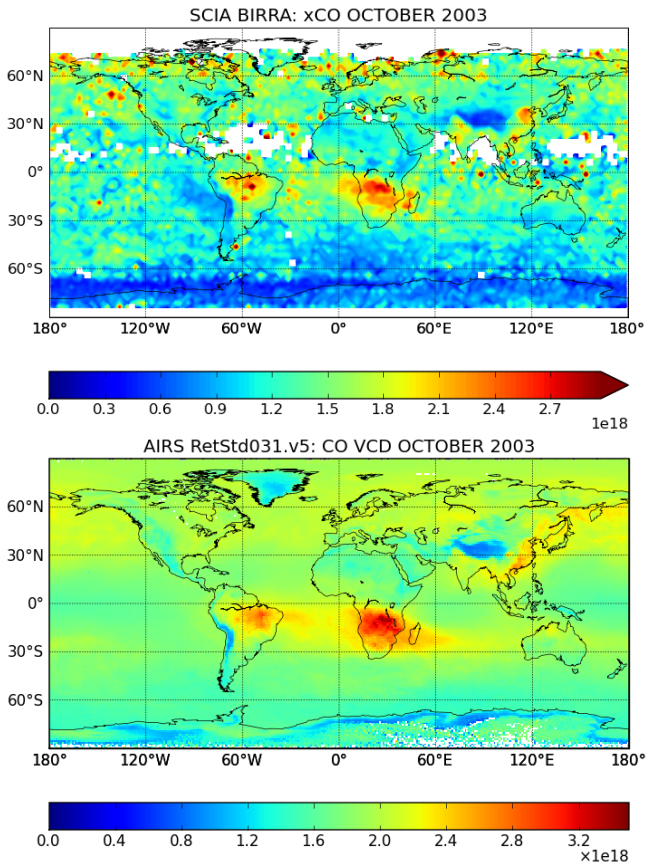

Figure 4. Comparison of October 2003 CO vertical column densities. (AIRS CO VCD represent the field "`CO_total_column_A`" of the official level 3 product version v.5.)

3.3. Results

In Fig. 4 a comparison of SCIAMACHY and AIRS monthly mean carbon monoxide vertical column densities for October 2003 are shown. Note that a single AIRS L1 granule has 9×1350 spectra, so an AIRS orbit gives more than 20 000 observations; On the other hand, a SCIAMACHY state typically consists of 260 spectra, resulting in about 2000 spectra per orbit.

The BIRRA results retrieved from SCIAMACHY represent the "dry air column density", i.e., CO VCD corrected by the scaling factor of methane considered here as a proxy for cloud fraction and cloud top height, scattering, instrument issues, and climatology. Single observations have been regridded and averaged into a $2.5^\circ \times 2.5^\circ$ global grid. The data has been filtered according to the following criteria:

- Convergence of the fitting algorithm
- Solar zenith angle smaller than 80°
- CO VCD positive and smaller than $1.5 \cdot 10^{19}\,\mathrm{cm}^{-2}$
- CH_4 scaling factor between 0.7 and 1.3.

No cloud filtering has been used. Along with the weak signal this is the main reason for the noisy data over the

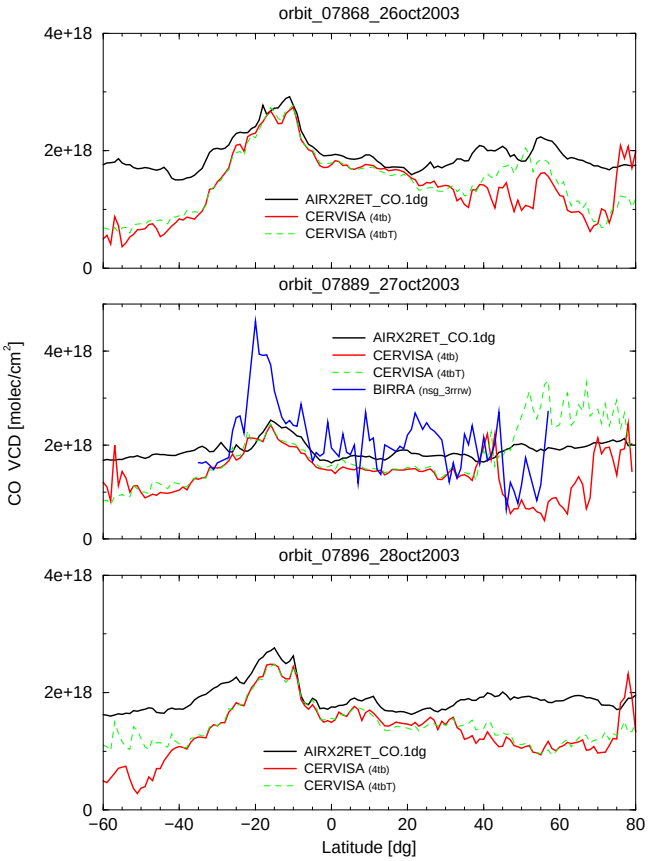

Figure 5. Comparison of CO vertical column densities as a function of latitude for three orbits end October 2003. For CERVISA 4 gases, surface temperature, and a constant baseline correction were fitted (label "4tb"), the "4tbT" curves show retrievals where the lowest level temperatures were adjusted to the surface temperature.

ocean. The noise at high latitudes is mainly due to the low signal in that regions.

Both products show enhanced CO densities over Southern Africa, the Amazonian region, and populated areas in East Asia. Moreover the SCIAMACHY—BIRRA results indicate high CO concentrations over Mumbay and the Ganges river valley.

In Fig. 5 results of CERVISA retrievals using AIRS L1 data (AIRIBRAD) from three orbits overpassing southeast Africa are compared with the "official" AIRS L2 data distributed by NASA (AIRX2RET). CO column densities (given as a function of latitude and longitude) have been averaged in 1dg latitude bins, with "bad" retrieval results (least squares return code indicating failure, $\mathrm{VCD_{CO}} > 10^{19}\,\mathrm{cm}^{-2}, \ldots$) filtered out. A series of CERVISA retrievals with slightly different settings had been performed (e.g., number of gases included, continuum on/off, baseline, ...), and including a constant baseline as further fit parameter turned out to be important. The enhanced CO emissions over Mozambique are clearly visible in all retrievals.

A reasonable good agreement between CERVISA and AIRX2RET is only found for low latitudes, whereas for high latitudes discrepancies become evident. Note that the AIRS L2 product indicates — on the average — increasing cloud coverage with increasing latitudes, however, CERVISA (and BIRRA) presently do not consider aerosols and clouds. As pressure and temperature usually were kept constant during the fit iterations, deviations from the actual conditions could also be responsible for these discrepancies. To test this assumption, retrievals were also performed where the lower troposphere temperature profile was adjusted according to the fitted surface temperature.

For October 27 the corresponding results derived from SCIAMACHY orbit 8663 are shown, too. The CO averaged over all longitudes within an 1dg latitude bin show larger scatter (see discussion above). The enhanced CO is significantly higher and slightly shifted to the south. Clearly a perfect match of AIRS and SCIAMACHY derived VCD's cannot be expected for several reasons, e.g., different altitude sensitivities of near and mid infrared spectra, SCIAMACHY daytime vs AIRS nighttime observation, slightly different spatial coverage, etc.

4. SUMMARY AND CONCLUSIONS

A new regularization scheme for nonlinear inverse problems based on Runge–Kutta methods has been implemented and tested with synthetic spectra for limb and nadir sounding. In comparison to other regularization schemes Runge–Kutta is less sensitive to the correct choice of the regularization parameter w.r.t. accuracy, albeit typically a higher number of iterations is required in case of bad parameter choice. For analysis of real measurement spectra the DRACULA library with Tikhonov-type and Runge–Kutta regularization schemes is currently combined with the MIRART/GARLIC radiative transfer code providing optimized line-by-line computations and algorithmic derivatives.

A modified version "CERVISA" of the "BIRRA" prototype of the operational SCIAMACHY near IR nadir level 2 processor has been implemented, and first results of carbon monoxide vertical column density retrievals from mid IR spectra have been shown. The CERVISA column densities were compared both with the official AIRS Level 2 product and with BIRRA results from SCIAMACHY observations. Ongoing work will focus on code optimization and investigation of further fit variables, nb. surface emissivity and atmospheric temperature.

ACKNOWLEDGMENTS

We would like to thank Michael Buchwitz and Heinrich Bovensmann (IUP, University of Bremen) for many helpful discussions and for providing SCIAMACHY level 1 and level 2 (WFM-DOAS)

data http://www.iup.uni-bremen.de/sciamachy/NIR_NADIR_WFM_DOAS/. Annemieke Gloudemans and Hans Schrijver (SRON, Utrecht) kindly delivered their SCIAMACHY carbon monoxide total column data. AIRS level 1, 2, and 3 data (v5) were retrieved from the NASA Langley Research Center Atmospheric Sciences Data Center.

REFERENCES

[1] C.D. Rodgers. *Inverse Methods for Atmospheric Sounding: Theory and Practise*. World Scientific, Singapore, 2000. 1

[2] A.N. Tikhonov. On the solution of incorrectly stated problems and a method of regularization. *Dokl. Acad. Nauk SSSR*, 151:501–504, 1963. 1

[3] B. Schimpf and F. Schreier. Robust and efficient inversion of vertical sounding atmospheric high–resolution spectra by means of regularization. *J. Geophys. Res.*, 102:16037–16055, 1997. 1

[4] P. Eriksson. Analysis and comparison of two linear regularization methods for passive atmospheric observation. *J. Geophys. Res.*, 105:18157–18167, 2000. 1

[5] O. Hasekamp and J. Landgraf. Ozone profile retrieval from backscattered ultraviolet radiances: The inverse problem solved by regularization. *J. Geophys. Res.*, 106:8077–8088, 2001. 1

[6] P.C. Hansen. *Rank–Deficient and Discrete Ill–Posed Problems: Numerical Aspects of Linear Inversion*. SIAM, Philadelphia, PA, 1998. 1

[7] T. Trucano and D. Post. Verification and validation in computational science and engineering. *Computing in Science & Engineering*, 6(5):8–9, 2004. 1

[8] Thomas von Clarmann, M. Höpfner, B. Funke, M. López-Puertas, A. Dudhia, V. Jay, F. Schreier, M. Ridolfi, S. Ceccherini, B.J. Kerridge, J. Reburn, and R. Siddans. Modeling of atmospheric mid–infrared radiative transfer: The AMIL2DA algorithm intercomparison experiment. *J. Quant. Spectrosc. & Radiat. Transfer*, 78:381–407, 2002. doi: 10.1016/S0022-4073(02)00262-5. 1, 3.1

[9] Thomas von Clarmann, S. Ceccherini, A. Doicu, A. Dudhia, B. Funke, U. Grabowski, S. Hilgers, V. Jay, A. Linden, M. López-Puertas, F.-J. Martín-Torres, V. Payne, J. Reburn, M. Ridolfi, F. Schreier, G. Schwarz, R. Siddans, and T. Steck. A blind test retrieval experiment for infrared limb emission spectrometry. *J. Geophys. Res.*, 108(D23):4746, 2003. doi: 10.1029/2003JD003835. 1

[10] A. Doicu, F. Schreier, and M. Hess. Iteratively regularized Gauss–Newton method for atmospheric remote sensing. *Comp. Phys. Comm.*, 148:214–226, 2002. doi: 10.1016/S0010-4655(02)00555-6. 2

[11] A. Doicu, F. Schreier, and M. Hess. Iteratively regularized Gauss–Newton method for bound–constraint problems in atmospheric remote sensing. *Comp. Phys. Comm.*, 153(1):59–65, 2003. doi: 10.1016/S0010-4655(03)00138-3. 2

[12] A. Doicu, F. Schreier, and M. Hess. Iterative regularization methods for atmospheric remote sensing. *J. Quant. Spectrosc. & Radiat. Transfer*, 83:47–61, 2004. doi: 10.1016/S0022-4073(02)00292-3. 2

[13] U. Tautenhahn. On the asymptotical regularization of nonlinear ill-posed problems. *Inverse Problems*, 10:1405–1418, 1994. 2.1

[14] C. Böckmann, , and P. Pornsawad. Iterative Runge-Kutta-type methods for nonlinear ill-posed problems. *Inverse Problems*, 2:025002, 2008. 2.1, 2.1

[15] H. Bovensmann, J.P. Burrows, M. Buchwitz, J. Frerick, S. Noël, V.V. Rozanov, K.V. Chance, and A.P.H. Goede. SCIAMACHY: Mission objectives and measurement mode. *J. Atmos. Sci.*, 56:127–150, 1999. 2.2, 3

[16] M. Buchwitz, I. Khlystova, H. Bovensmann, and J. P. Burrows. Three years of global carbon monoxide from SCIAMACHY: comparison with MOPITT and first results related to the detection of enhanced CO over cities. *Atm. Chem. Phys.*, 7:2399–2411, 2007. 3

[17] C. Frankenberg, U. Platt, and T. Wagner. Iterative maximum a posteriori (IMAP)-DOAS for retrieval of strongly absorbing trace gases: Model studies for CH_4 and CO_2 retrieval from near infrared spectra of SCIAMACHY onboard ENVISAT. *Atm. Chem. Phys.*, 5:9–22, 2005. 3

[18] A.M.S. Gloudemans, H. Schrijver, O.P. Hasekamp, and I. Aben. Error analysis for CO and CH_4 total column retrievals from SCIAMACHY 2.3 μm spectra. *Atm. Chem. Phys.*, 8:3999–4017, 2008. 3

[19] F. Schreier, S. Gimeno-Garcia, M. Hess, A. Doicu, A. von Bargen, M. Buchwitz, I. Khlystova, H. Bovensmann, and J.P. Burrows. Intercomparison of vertical column densities derived from SCIAMACHY infrared nadir observations. In H. Lacoste and L. Ouwehand, editors, *Proceedings of Envisat Symposium 2007*, volume SP-636. ESA, July 2007. 3

[20] F. Schreier, S. Gimeno-Garcia, M. Hess, A. Doicu, and G. Lichtenberg. Carbon monoxide vertical column density retrieval from sciamachy infrared nadir observations. In T. Nakajima and M. A. Yamasoe, editors, *Current Problems in Atmospheric Radiation (IRS 2008)*, volume CP1100. American Institute of Physics, 2009. doi: 10.1063/1.3116983. 3

[21] J.E. Dennis, Jr., D.M. Gay, and R.E. Welsch. An adaptive nonlinear least–squares algorithm. *ACM Trans. Math. Soft.*, 7:348–368, 1981. 3

[22] F. Schreier and B. Schimpf. A new efficient line–by–line code for high resolution atmospheric radiation computations incl. derivatives. In W.L. Smith and Y. Timofeyev, editors, *IRS 2000: Current Problems in Atmospheric Radiation*, pages 381–384. A. Deepak Publishing, 2001. 3.1

[23] A. Griewank. *Evaluating Derivatives: Principles and Techniques of Algorithmic Differentiation*. SIAM, Philadelphia, PA, 2000. 3.1

[24] C. Melsheimer, C. Verdes, S.A. Bühler, C. Emde, P. Eriksson, D.G. Feist, S. Ichizawa, V.O. John, Y. Kasai, G. Kopp, N. Koulev, T. Kuhn, O. Lemke, S. Ochiai, F. Schreier, T.R. Sreerekha, M. Suzuki, C. Takahashi, S. Tsujimaru, and J. Urban. Intercomparison of general purpose clear sky atmospheric radiative transfer models for the millimeter/submillimeter spectral range. *Radio Science*, 40: RS1007, 2005. doi: 10.1029/2004RS003110. 3.1

[25] Kuo-Nan Liou. *An Introduction to Atmospheric Radiation*. Academic Press, Orlando, 1980. 3.1

[26] W. W. McMillan, C. Barnet, L. Strow, M. T. Chahine, M. L. McCourt, J. X. Warner, P. C. Novelli, S. Korontzi, E. S. Maddy, and S. Datta. Daily global maps of carbon monoxide from NASA's Atmospheric Infrared Sounder. *Geophys. Res. Letters*, 32:L11801, 2005. doi: 10.1029/2004GL021821. 3.2

[27] Eric L. Fleming, Sushil Chandra, J. J. Barnett, and M. Corney. Zonal mean temperature, pressure, zonal wind and geopotential height as functions of latitude. *Adv. Space Res.*, 10(12):11–59, 1990. doi: 10.1016/0273-1177(90)90386-E. 3.2

[28] G.P. Anderson, S.A. Clough, F.X. Kneizys, J.H. Chetwynd, and E.P. Shettle. AFGL atmospheric constituent profiles ($0 - 120\,\mathrm{km}$). Technical Report TR-86-0110, AFGL, 1986. 3.2

[29] L.S. Rothman et al. The HITRAN 2004 molecular spectroscopic database. *J. Quant. Spectrosc. & Radiat. Transfer*, 96:139–204, 2005. 3.2